

FINAL PROJECT

Aim: Classification of galaxies with emission lines

Side-aims: Improvement of programming, data analysis, data representation skills, paper writing

Points: 25

Hard deadline: May 31st; 2023;

Soft deadline (points scaled with 0.7): June 15th 2023

Classifications of emission-line galaxies using SDSS and WISE surveys

With on-going and coming large surveys one of the most important tasks is the classification of detected objects. In case of galaxies with emission lines in their spectra, the general problem is how one can reliably classify a galaxy as a starburst galaxy or an active galactic nuclei (AGN). The best way is to provide a classification that is based on different “excitation” mechanism in these objects. That is what BPT diagrams are doing.

“Baldwin, Phillips & Terlevich” (BPT 1981) diagrams demonstrate how LINERs can be distinguished from normal H II regions and normal AGNs (Seyferts and QSOs) on the basis of their [O III] $\lambda 5007$, H β , [N II] $\lambda 6583$, H α , [O I] and [S II] $\lambda\lambda 6716, 6731$ / H α flux ratios. It is basically the way how to distinguish between the starburst galaxies and AGN.

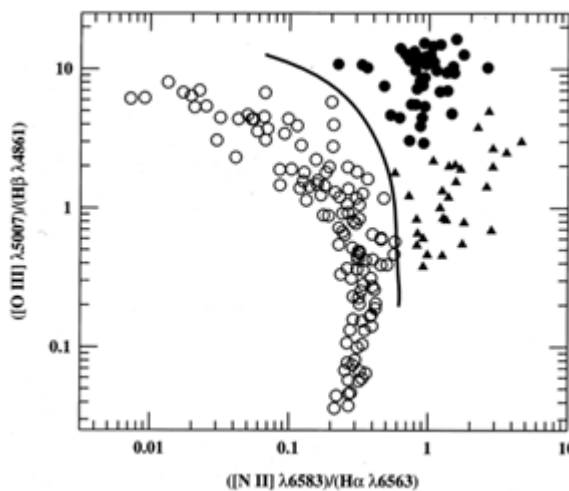


Figure 1. Here it is seen that the Seyfert 2s have high values of each ratio (*open circles are for H II regions and similar sources that are clearly ionized by hot stars; closed circles are narrow-line AGNs (Seyfert 2s and NLRGs) which are ionized by “harder” continua (i.e. with a greater fraction of high-energy photons, such as a power-law spectrum); solid line is an empirical division between these two classes of object; triangles represent LINERs*). H II regions define a locus of lower values which does not overlap with the

region of parameter space occupied by the Seyferts. The LINERs can be distinguished from the Seyfert 2s by their low values of [O III] $\lambda 5007$ / H β relative to [N II] $\lambda 6583$ / H α , and from the H II regions by their larger values of [N II] $\lambda 6583$ / H α .

Another more comprehensive emission-line classification of SDSS galaxies is based on the equivalent width of H α ($W_{H\alpha}$) versus [N II]/H α diagram (so-called WHAN diagram, Figure 2), proposed by Cid Fernandes et al. (2011). This classification can cope with the weak line galaxies that do not appear in traditional diagrams due to a lack of some of the diagnostic lines. Also, WHAN diagram allows the differentiation between two very distinct classes of the low-ionization nuclear emission-line region (LINER) objects: galaxies hosting a weakly active galactic nucleus (wAGN) and 'retired galaxies' (RGs), i.e. galaxies that have stopped forming stars and are ionized by their hot low-mass evolved stars. Based on the bimodal distribution of $W_{H\alpha}$, we set the practical division between wAGN and RGs at $W_{H\alpha} = 3 \text{ \AA}$. There are five classes of galaxies identified within the WHAN diagram:

- (i) pure star-forming galaxies: $\log ([\text{N II}]/\text{H}\alpha) < -0.4$ and $W_{H\alpha} > 3 \text{ \AA}$;
- (ii) strong AGN (i.e. Seyferts): $\log ([\text{N II}]/\text{H}\alpha) > -0.4$ and $W_{H\alpha} > 6 \text{ \AA}$;
- (iii) weak AGN: $\log ([\text{N II}]/\text{H}\alpha) > -0.4$ and $W_{H\alpha}$ between 3 and 6 \AA ;
- (iv) RGs (i.e. fake AGN): $W_{H\alpha} < 3 \text{ \AA}$;
- (v) passive galaxies (actually, lineless galaxies): $W_{H\alpha}$ and $W_{[\text{N II}]}$ $< 0.5 \text{ \AA}$.

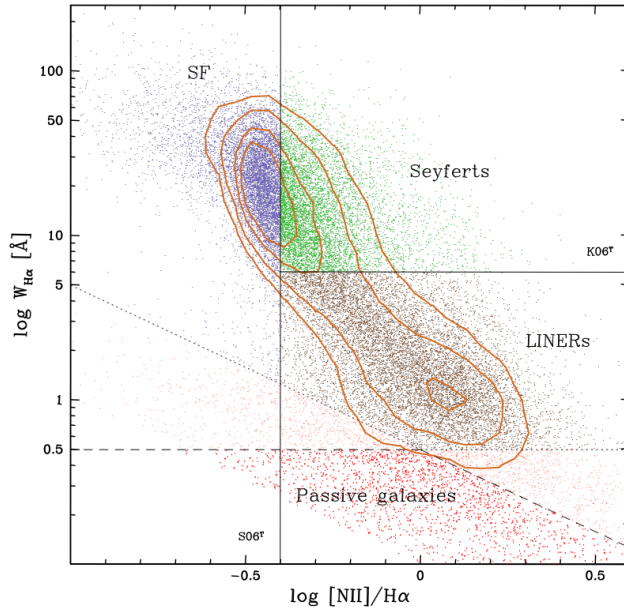
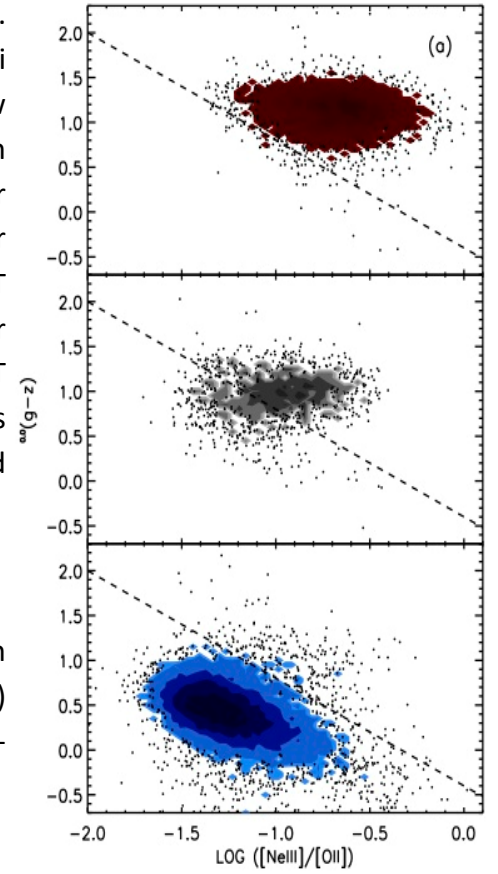


Figure 2: WHAN diagram from Cid Fernandes et al. (2011). The line labelled $S06^T$ represents the optimal transposition of the BPT-based SF/AGN division, while the line at $W_{H\alpha} = 6 \text{ \AA}$ represents the transposed version of the Kewley et al. (2006) Seyfert/LINER class division. Dotted lines mark $W_{H\alpha} = 0.5$ and $W_{[\text{N II}]} = 0.5 \text{ \AA}$ limits, below which line measurements are uncertain. Passive galaxies ($W_{H\alpha}$ and $W_{[\text{N II}]} < 0.5 \text{ \AA}$; red dots) lie below the dashed line.

The BPT diagram in general works well, but one problem is when we need to classify galaxies that are farther away (at higher redshift, z), as then the emission lines needed to make a BPT diagram quickly shift out of the optical window into the infrared, where getting spectra is much harder. In fact, beyond $z > 0.4$, the BPT diagram can no longer be used.

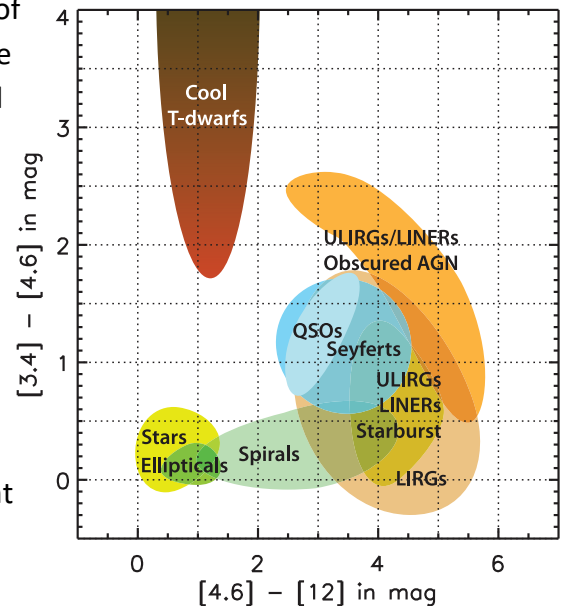
Therefore, there is a need for other diagnostics diagrams. One possibility is given by Trouille, Barger & Tremonti (2011) - TBT 2011. These authors have created a new diagnostic, similar to the BPT diagram, but which relies on the emission lines [NeIII] and [OII] that are at shorter wavelengths, and uses a completely different feature for the y-axis – restframe (g-z) color (see Figure 3, from TBT 2011). The authors call this the TBT diagram, and in their paper, they show that it works just as well as the BPT diagram to separate star-forming galaxies from AGN, is actually better at finding AGN that are X-ray obscured, and best of all, can be used out to $z=1.4$.

Figure 3: The "TBT" diagram, which uses the NeIII to OII ratio and (g-z) color to classify objects as AGN or star-forming galaxies (from TBT 2011).



In addition, the mid-infrared colors can be used to identify the presence of AGN-heated dust in the spectral energy distributions of galaxies. For this, one can use the Wide-field Infrared Survey Explorer (WISE) which has scanned the night sky in four bands (3.4, 4.6, 12, and 22 μm , W1,W2,W3,W4), to classify different classes of extragalactic objects through MIR WISE colors (Figure 4). For example, Mateos et al. (2012) have suggested a highly complete and reliable technique to select luminous AGN using WISE colors, as well as that this technique can be used to identify obscured AGN missed in X-ray surveys (Mateos et al. 2013).

Figure 4: WISE colours diagram. Regions with different color shading show typical MIR colors of different populations of objects (Wright et al. 2010).



TASK 1:

The first and main project task is to **extract top 30,000 galaxies** with **narrow emission lines** with redshift $z < 0.3$ from the SDSS database (e.g. DR17 or DR18 –<http://www.sdss.org/>) using the SQL search and produce BPT diagram.

Obtain the following line fluxes **[O III] $\lambda 5007$, $H\beta$, [N II] $\lambda 6583$, $H\alpha$, [S II] $\lambda\lambda 6716, 6731$, [O I] $\lambda 6300$** , and **equivalent width of $H\alpha$** from the SDSS spectral databases (tips: *when selecting galaxies define as one of the criteria that you only need narrow emission line; find a way to calculate line fluxes using only data available in SDSS tables*). For the division line use the theoretical curves obtained by Kewley et al. (2001) and empirical curves from Kauffman et al. (2003). Make plots for **[O III] $\lambda 5007/H\beta$ vs. [N II] $\lambda 6583/H\alpha$** , denoting with different marks/colors different object (e.g. as shown in Figure 5).

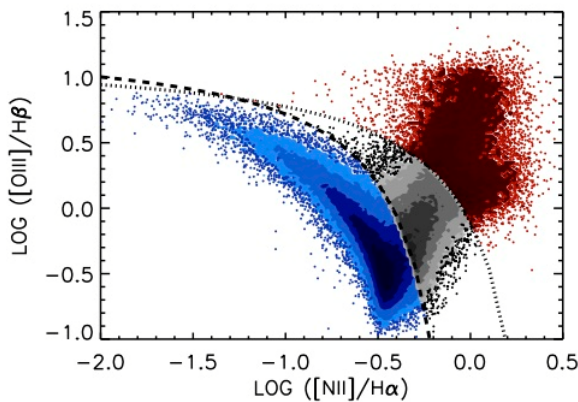


Figure 5: Galaxies (blue), composites (grey), and AGN (red) separated on the traditional BPT diagram (from TBT 2011).

TASK 1a:

Test the classification obtained using the first BPT diagnostics **[O III] $\lambda 5007/H\beta$ vs. [N II] $\lambda 6584/H\alpha$** , with the other two common BPT diagnostic tools: 1) **[O III] $\lambda 5007/H\beta$ vs. [S II] $\lambda\lambda 6716, 6731/H\alpha$** , 2) **[O III] $\lambda 5007/H\beta$ vs. [O I] $\lambda 6300/H\alpha$** . (Tip: use the same mark/color notation as for the first diagnostic in order to be able to make comparison).

TASK 1b:

Make a WHAN diagram, the **equivalent width of $H\alpha$ ($W_{H\alpha}$) vs. [N II]/ $H\alpha$ ratio**, for the objects already classified (keep the same notation, i.e. the classification information obtained in the BPT diagram). Comment and discuss the obtained results, **give the number/percentage of objects classified as (strong) AGN/Seyferts by the BPT and WHAN diagrams**.

TASK 2:

For a subsample of these SDSS objects, there are also [Ne III] $\lambda 3869$ and [O II] $\lambda\lambda 3726, 3729$ line fluxes available (*tip: set S/N ratio to at least 5*). Extract that subsample from the first sample, together with their g, z magnitudes and above line fluxes. Make the BPT and TBT diagrams for this subsample, keeping the same notation (i.e. use the classification information obtained in the BPT diagram for the TBT diagram). The observed magnitudes should be transformed to the z=0 frame using k-correction (Chilingarian et al. 2010, website: <http://kcor.sai.msu.ru/> or Blanton & Roweis 2007, website: <http://howdy.physics.nyu.edu/index.php/Kcorrect>).

The division line on the TBT diagram is as follows:

$$(g-z)_0 = -1.2 \times \log([NeIII]/[OII]) - 0.4$$

where $(g-z)_0$ is the rest-frame g-z color, [NeIII] is the line flux of [Ne III] $\lambda 3869$ and [OII] is the line flux of the [OII] $\lambda\lambda 3726, 3729$ doublet (sometimes labeled as [OII] $\lambda 3727$ when the doublet components are not resolved).

Comment on what is the number/percentage of objects defined as AGN by BPT, TBT and both BPT and TBT diagrams.

TASK 3:

For sample of AGN selected from the SDSS database, find the WISE counterparts with a matching tolerance of 3'' ($\sim 0.5 \times \text{FWHM}$ of the WISE PSF at 3.4 μm), and get the three WISE colors (W1, W2, W3). Locate the object on the WISE colour-colour plot using the selection criteria defined by Mateos et al. (2012, 2013):

$$\begin{aligned} y &= 0.315 \times x \\ x &\equiv \log_{10}(f_{12\mu\text{m}}/f_{4.6\mu\text{m}}) \\ y &\equiv \log_{10}(f_{4.6\mu\text{m}}/f_{3.4\mu\text{m}}) \end{aligned}$$

The top and bottom boundaries of the wedge are obtained by adding y-axis intercepts of +0.297 and -0.110, respectively. The MIR power-law $\alpha = -0.3$ bottom-left limit corresponds to:

$$y = -3.172 \times x + 0.436$$

Plot your results on top of the Figure 12 taken from Wright et al. (2010).

Comment on what is the percentage of object found in both SDSS and WISE survey, what is the number/percentage of objects defined as AGN by SDSS and WISE, as well as what is the number/percentage of objects found to be AGN by both surveys.

In your report, explain all the steps you have taken, and provide complete tables and computer codes in the Appendix of the report.

REFERENCES and HELP:

Baldwin, J. A., Phillips, M. M., & Terlevich, R. 1981, PASP, 93, 5 (BPT 1981)
Blanton, M. R., & Roweis, S. 2007, AJ, 133, 734
Calzetti, D., et al., 2007, ApJ, 666, 870
Chilingarian, I., Melchior, A.-L., Zolotukhin, I. 2010, MNRAS, 405, 1409
Cid Fernandes, R. et al. 2011, MNRAS, 413, 1687
Hogg 2000, Distance measures in cosmology, arXiv:astro-ph/9905116
Kewley et al. (2001), ApJ 556, 121
Kauffman et al. (2003), MNRAS 346, 1055
Mateos, S. et al. (2012), MNRAS, 426, 3271
Mateos, S. et al. (2013), MNRAS, 434, 941
Trouille, L., Barger, A.J., & Tremonti, C. (2011), ApJ, 742, 46 (TBT 2011)
Wright et al. (2010), ApJ, 140, 1868

Program for plotting - GNUPLOT: <http://www.gnuplot.info/>

LaTeX – a document preparation system <http://www.latex-project.org/intro.html>

SciPython – <http://www.scipy.org/>

k-correction: <http://howdy.physics.nyu.edu/index.php/Kcorrect>, <http://kcor.sai.msu.ru/>